Optics Communications 281 (2008) 5771–5774

Contents lists available at ScienceDirect

Optics Communications

journal homepage: www.elsevier.com/locate/optcom

One-dimensional coupled cavities photonic crystal filters with tapered Bragg mirrors

Qin Chen *, Duncan W.E. Allsopp

Department of Electronic and Electrical Engineering, University of Bath, Bath BA2 7AY, United Kingdom

ARTICLE INFO

Article history:
Received 16 June 2008
Received in revised form 14 August 2008
Accepted 15 August 2008

Keywords:
Filters
Photonic crystal
Microresonators
Gratings
Finite difference methods

ABSTRACT

The performance of one-dimensional (1D) coupled cavities photonic crystal (PC) filters has been analyzed by finite-difference time-domain (FDTD) simulation. It is shown that the addition of tapered Bragg mirrors at each side of the cavities, to create near-Gaussian field profiles for the cavity modes, results in the prediction of near flat-top passband filters with high out-of-band rejection ratio and near unity transmission. The tapered structures suppress the vertical radiation loss to allow optimization of the number of mirror periods for the best filter response whilst guaranteeing high transmission. A critical coupling condition ($k = 2L_{out}/L_{in} = 1$) for flat-top responses in doubly coupled cavities filters is proposed in the tapered structures. An optimized filter for 100 GHz optical communication system are demonstrated with 1 dB bandwidth of 0.17 nm, roll-off of 0.6 dB/GHz, out-of-band signal rejection of 33 dB and transmission of 95%. Further improvement of roll-off and out-of-band rejection is demonstrated in a triply coupled cavities filter.

1. Introduction

Selective bandpass filters play a vital role in modern dense wavelength-division multiplexing (DWDM) systems that are characterized by small channel spacing and high bit rates [1]. There are numerous technologies for realizing bandpass filters. Dielectric thin-film [2], arrayed-waveguide grating [3], and Mach–Zehnder [4] filters are mature technologies but their complexity or dimensions strongly increase for applications in DWDM systems. As an emerging technology, microcavity filters have the great advantage of compact size, a requirement for high density photonic integration. Other major advantages include high finesse, which guarantees the separation of two adjacent channels and low cross talk, and a large free spectral range, which ensures the clean transfer of a single channel to and from the whole DWDM band [5–14].

Compared to microring/microdisk filters, PC cavity filters are even more compact, have higher quality factors (Q-factors) and more flexibility in the design [9–14]. Filters made in 2D PC slabs have been the subject of much attention [10,11,13], owing to the development of ultrahigh-Q microcavities [15]. One-dimensional (1D) PC wavelength selective structures, i.e. Bragg gratings embedded in optical waveguides or fibers, have been largely demonstrated and discussed due to the advantages in terms of simplicity and flexibility [16–19]. Recently, a 1D PC filter with tapered Bragg mirrors in a silicon-on-insulator (SOI) waveguide with a Q-factor as high as 8900 and a transmission of 60% was demonstrated [20], showing the potential of such structures for applications in photonic integrated circuits.

In our most recent paper [21], a 1D PC cavity with tapered Bragg mirrors demonstrated an ultrahigh-Q (>6.7×10^6) resonance, in which the optimized Gaussian-like mode field distribution suppresses the out-of-plane loss. However, the intrinsic Lorentzian filtering response in a single cavity PC filter is not ideal for practical applications. For densely spaced channels, the desired filter characteristic is a box-like response with a flat passband and fast roll-off. High-order filters, i.e. coupled cavity filters, have been widely investigated for engineering the filtering response [6,8,10–12,22,23]. Higher-order filters have a larger out-of-band rejection and a steeper slope. In the case of coupled cavity filters, the shape of the passband depends on the number of Bragg mirror periods in the inner and outer reflectors [23]. However, the out-of-plane radiation loss is larger when longer gratings are used to increase Q-factor or when complex PCs are used to create the filtering function [14], limiting the scope for optimizing the shape of the passband. This is a more serious problem in SOI materials where the large index contrast can increase the loss to limit the linewidth of the spectral response [10].

This paper describes an investigation by FDTD method of high-order 1D PC filters with tapered Bragg mirrors. The critical coupling condition is presented for second order filters with flat-top spectral responses. The innovation of using tapered Bragg mirrors is shown to enable the formation of a second order filter with 1 dB bandwidth of 0.17 nm, roll-off of 0.6 dB/GHz, out-of-band rejection of 33 dB and transmission of 95%.

* Corresponding author.
E-mail address: qc206@bath.ac.uk (Q. Chen).

0030-4018/$ - see front matter © 2008 Elsevier B.V. All rights reserved.
doi:10.1016/j.optcom.2008.08.023

2. Method

Transfer-matrix-method (TMM) is a conventional and efficient method for the analysis of optical gratings [12,14,22,23]. However, it does not take into account the out-of-plane loss, which is the key parameter in PC cavity and waveguide structures in micro-scale. Actually, the loss becomes the determinate factor in such a structure in SOI materials, where the refractive index contrast is large and the light scattering is not negligible.

FDTD method has been proved to be the most accurate numerical method for the optical waveguide investigation [5,7–11]. Being named as a numerical experiment, FDTD includes all loss mechanism in the simulation and provides the closest result to the real world. In this paper, FDTD method is used in the filtering response simulation as in [7,21].

The schematic of a second order 1D PC filter based on doubly coupled cavities is shown in Fig. 1. It comprises a block of SOI material consisting of a Si substrate, SiO_2 buffer layer of 1.5 μm, the top Si guide layer of 360 nm and the air cladding layer. The refractive index values of silicon and silicon dioxide used in the calculations are 3.48 and 1.46, respectively. It is assumed that coupled cavities layers are then formed by etching Bragg mirrors, where $N_{\text{inner}} + ½$ pairs of Si and air gap layers are sandwiched between two coupled cavities with thickness D and $N_{\text{outer}} + ½$ pairs of Si and air gap layers between the cavities and the feeder waveguides.

In the 2D FDTD simulations, the corrugated waveguide is assumed to be illuminated from the input waveguide by the transverse magnetic (TM, $H_y = 0$) fundamental mode, which is a Gaussian-modulated cosine impulse covering a wide frequency band. The "bootstrapping" technique is used to set the exciting source [24]. The perfectly matched layer (PML) absorbing boundary is used to terminate the FDTD calculation window, with the PML thickness of 0.5 and 1 μm in the x and z directions, respectively. The spatial cell size is 10 nm, and the time step is Courant limit [24]. The transmission spectra are calculated from the power flux recorded at the detector plane, which is normalised by the source value. The resonance wavelength is found by fitting a Lorentzian to the transmission peak and Q-factor is given by the ratio of the peak wavelength to its 3 dB bandwidth. By compressing the incident impulse spectral width into a range narrow enough to ensure that only on-resonance modes can be excited, we can obtain the mode field distributions from the FDTD simulation.

3. Filtering response in second order PC filters

In Ref. [21], it is shown that tapered mirrors formed by varying the length of Si blocks close to the cavity layer creates a nearly ideal field profile in a single microcavity and suppresses the vertical radiation loss, to yield a theoretical Q-factor as high as 6.7×10^6. In this paper, the widths of Si block dH, air gap dL and the cavity D are set to be the same values as in [21], namely 200 nm, 90 nm and 400 nm, respectively. The etch depth h is set to be 650 nm. Si tapers are added to the Bragg reflectors by reshaping the three Si blocks in each mirror closest to the cavity layer so that their widths decrease from 170 to 190 nm, in steps of 10 nm, moving away from the cavity while the air section lengths remain constant. Fig. 2 shows the effect of the number of complete mirror pairs N_{inner} and N_{outer} on the performance of the filter. In all cases N_{outer} includes the number of the tapered periods and the responses for $N_{\text{outer}} = 5$, 6 and 7 are shown respectively in Fig 2a–c. The values of N_{inner} are given by $N_{\text{inner}} = 2N_{\text{outer}} + s$ where $s = -1$, 0, +1, +2 for each value of N_{outer} considered.

The grating section between the coupled cavities has a strong influence on the filtering response. In each case, a top-flat filtering

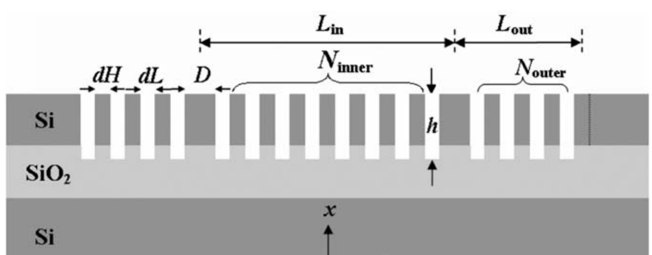

Fig. 1. Schematic of a second order 1D PC filter on SOI material ($N_{\text{inner}} = 7$, $N_{\text{outer}} = 3$).

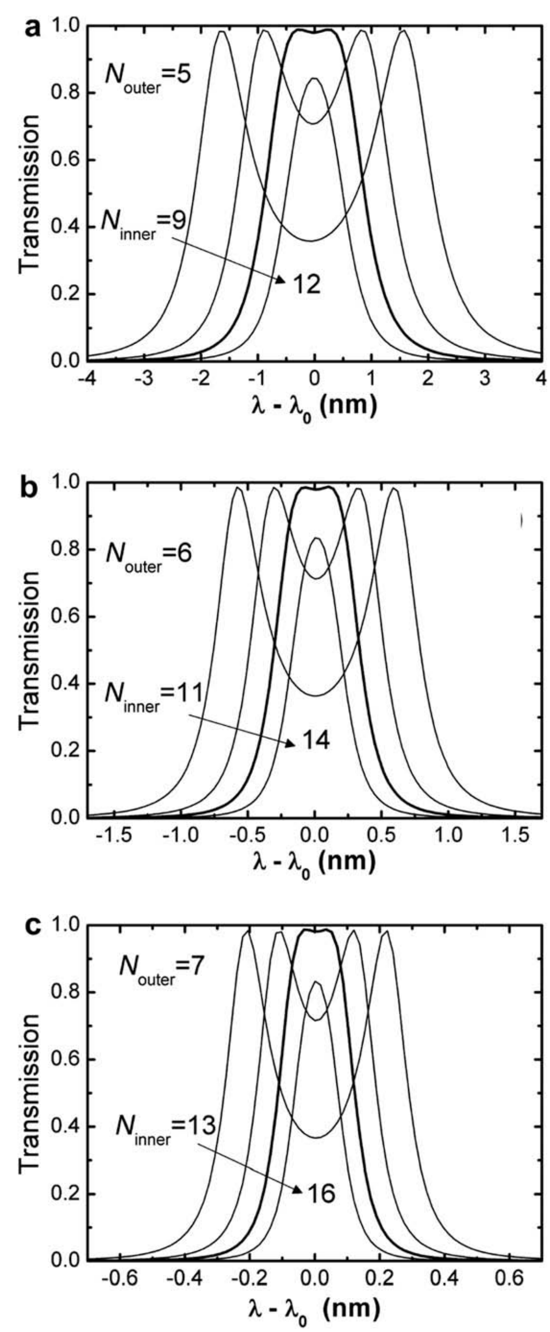

Fig. 2. Spectra responses of second order PC filters with tapers. (a) $N_{\text{outer}} = 5$ (including the tapers), (b) $N_{\text{outer}} = 6$, (c) $N_{\text{outer}} = 7$. The spectra at $N_{\text{inner}} = 2, N_{\text{outer}} + 1$, i.e. $k = 1$, are plotted as thick solid lines.

response is observed at $N_{\text{inner}} = 2N_{\text{outer}} + 1$. When N_{inner} is less than this critical value for flat responses, two peaks appear in the response due to the strong coupling. The resonant modes in two isolated cavities couple with each other and their wavelengths shift from the initial wavelength λ_0. Decreasing N_{inner} increases the coupling strength, causing a larger wavelength shift and hence a deeper dip in the spectral response. When N_{in} is larger than the critical value, the coupling between the two cavities becomes weaker and no obvious wavelength shift occurs. The filtering behavior of the whole structure becomes that of a series of filters of the same selective wavelength and has a Lorentzian shape with reduced transmission. Based on the results in Fig. 2, a top-flat filtering response can be realized in a 1D second order PC filter at $N_{\text{in}} = 2N_{\text{out}} + 1$. For further analysis, we define $k = 2L_{\text{out}}/L_{\text{in}}$, where L_{in} is the center-to-center distance between the two cavities and L_{out} is the distance from the center of one cavity to the plane with dH/2 length into the feed waveguide as marked in Fig. 1. So $k = 1$ is found to be the critical condition for a top-flat response. This result confirms extends the finding in [22] based on a transfer matrix method that neglects the effect of vertical radiation loss on the transmission and the full-width at half-maximum (FWHM).

The filtering responses at $k = 1$ in both tapered and non-tapered 1D PC filters are shown in Fig. 3 for different N_{outer}. For the non-tapered structures shown in Fig. 3a, the FWHM of the passband decreases significantly with the increasing N_{outer} but at the cost of degraded transmission. For example, only 40% transmission occurs when $N_{\text{outer}} = 8$. Consequently, in any practical application the compression of the FWHM achieved by increasing N_{outer} will be limited by the transmission value. Fig. 3b shows the effect of adding tapers between the cavities and the outer Bragg mirrors. As N_{outer} varies from 4 to 8, the FWHM is compressed from 4.9 nm to 0.085 nm. However, with the tapers added the flat-top transmission remains above 98%. As discussed in [21], optimum tapers give rise to cavity modes with a Gaussian-like field distribution and suppresses the vertical radiation loss, enabling the use of longer Bragg mirrors to tailor the passband to meet a given system specification.

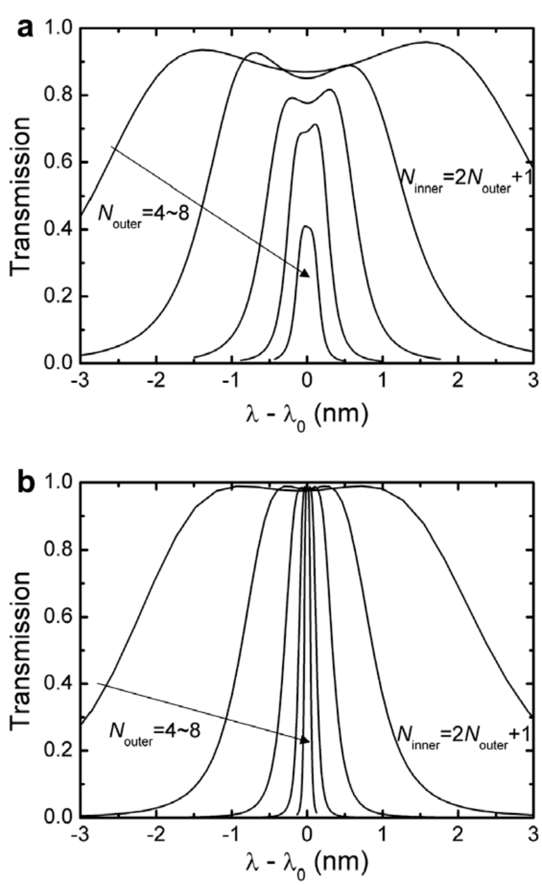

Fig. 3. (a) Spectra responses of second order PC filters without tapers. (b) Spectra responses of second order PC filters with tapers. In both cases, $N_{\text{inner}} = 2$, $N_{\text{outer}} + 1$, i.e. $k = 1$, and N_{outer} varies from 4 to 8.

For example, a second order 1D PC microcavity filter with $N_{\text{outer}} = 7$ and $k = 1$ will meet the requirements of a DWDM system operating at 100 GHz, i.e. 0.8 nm channel interval. This is shown in Fig. 4 which compares the spectral response of both non-tapered and tapered first and second order PC filters. Compared to the Lorentzian filtering responses of single cavity filters, the second order filters have flat transmission bands with steep roll-off. Defining the signal out-of-band rejection as the ratio of spectral intensity at central wavelength and 0.8 nm-offset wavelength, we summarize the filtering characteristics in single cavity filters with and without tapers, and second order filters with and without tapers in Table 1. It is obvious that the second order filter with tapered structures supports the highest transmission of 95%, the maximum out-of-band rejection of 33 dB, and has the largest roll-off of 0.6 dB/GHz. Such a filter will greatly reduce crosstalk between neighboring channels in DWDM systems.

The −1 dB bandwidth is 0.17 nm in the tapered second order filter, which corresponds to a 20 GHz modulation bandwidth. In the case of a tapered single cavity filter, a 30 dB out-of-band rejection occurs only with a −1 dB bandwidth of 0.02 nm, owing to the Lorentzian shape of its response, a value too low to accommodate encoding a high data rate on to an optical carrier. In addition, the FWHM in this tapered second order filter will in fact be smaller than that of the first order filter, unlike the results in [10] where the FWHM significantly increases in second order filters. This result demonstrates the feasibility of such a 1D PC filter for application in DWDM systems.

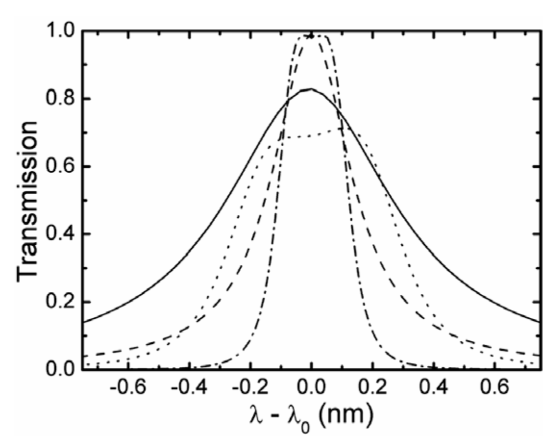

Fig. 4. Spectra responses in a single cavity PC filter without (solid line) and with (dashed line) tapers, and in the corresponding second order filters without (dotted line) and with (dash dot) tapers, where $N_{\text{outer}} = 7$.

Table 1
Filtering characteristics in single cavity filters with (ST) and without (S) tapers, and doubly coupled cavities filters with (DT) and without (D) tapers

	S	ST	D	DT
Roll-off (dB/GHz)	0.09	0.19	0.25	0.60
Signal rejection (dB)	8	14	17	33
−1 dB Band width (nm)	0.34	0.15	0.42	0.17
Transmission in −1 dB band	80%	95%	69%	95%

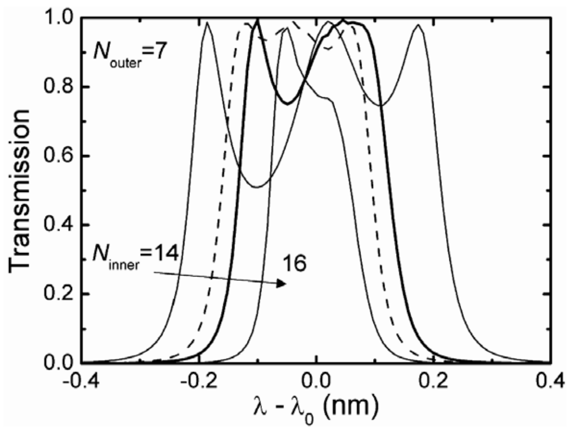

Fig. 5. Spectra responses of third order PC filters with tapers, where *N*outer = 7 and *N*inner varies from 14 to 16. The response in an optimized third order filter is shown as dashed line.

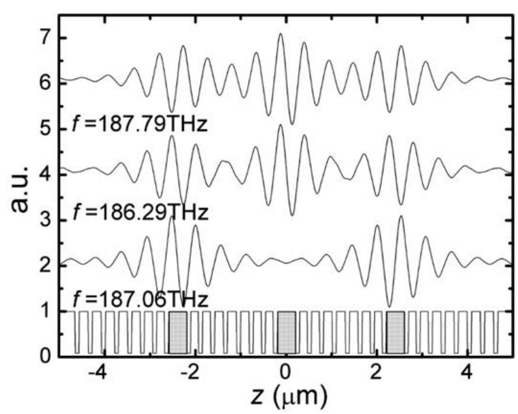

Fig. 6. Electric field and the refractive index distribution in the third order PC filter at *N*outer = 7 and *N*inner = 7. Two anti-symmetrical modes *f* = 186.29, 187.79 THz and one symmetrical mode *f* = 187.06 THz are shown.

4. Filtering response in third order PC filters

Further improvements of the out-of-band rejection and the roll-off are expected in higher-order filters as discussed in [22,23]. The spectral response of third order 1D PC filters with the same tapered structure parameters are shown in Fig. 5 for $N_{outer} = 7$. The optimized response is again found at $N_{inner} = 2N_{outer} + 1$, although the peak response now is not as flat as for the optimum second order filters shown in Fig. 2. The −1.2 dB bandwidth is 0.23 nm. However, the roll-off is almost double that of the optimum second order filter and the out-of-band rejection increases to 50 dB. Based on TMM simulation, we found that the non-symmetry and non-flat top at $k = 1$ are caused by the non-π phase shift in each pair of Bragg mirror. In fact, the resonant mode in each isolated single cavity should be on resonance. As these three cavities couple with each other, the modes shift in frequency and raise a wider flat-top rather than a Lorentzian shape. The field distributions of three resonant modes in the whole structure are shown in Fig. 6 together with the refractive index distribution. A simple optimization of the filtering response is demonstrated in Fig. 5 as dashed line, where an increase of the refractive index of the central cavity as small as 2×10^{-4} relative to the outer cavities is introduced. Such a small refractive index change can be achieved by carrier injection in Si. The frequency intervals between three resonator modes are engineering slightly and give a more flat top of the spectral response. A further improvement in the third order filters is expected as TMM predicts if high Si-filling ratio Bragg mirrors with π phase shift is used.

5. Conclusion

In conclusion, high-order 1D PC filters with tapered Bragg mirrors have been investigated by FDTD method. The effect of the numbers of mirror pairs N_{inner} and N_{outer} on the performance of the filters is discussed in detail and $N_{inner} = 2N_{outer} + 1$ is found to be the critical coupling condition for a flat-top response in second order filters. The use of outer Bragg mirrors that incorporate tapers results in flat passbands with transmission above 95%. In particular, the FWHM of an optimized spectral response is reduced to 0.22 nm with a roll-off of 0.6 dB/GHz and an out-of-band rejection of 33 dB. Higher-order structures such as third order filters demonstrate larger roll-offs and out-of-band rejections. Such compact 1D PC filters offer major opportunities for realizing photonic integrated circuits for application in future DWDM systems.

References

[1] C.K. Madsen, J.H. Zhao, Optical Filter Design and Analysis: A Signal Processing Approach, Wiley, New York, 1999.
[2] J. Minowa, Y. Fujii, J. Lightwave Technol. 1 (1983) 116.
[3] M.K. Smit, C. van Dam, IEEE J. Sel. Top. Quantum Electron. 2 (1996) 236.
[4] M. Kuznetsov, J. Lightwave Technol. 12 (1994) 226.
[5] B.E. Little, S.T. Chu, H.A. Haus, J. Foresi, J.-P. Laine, J. Lightwave Technol. 15 (1997) 998.
[6] A. Melloni, M. Martinelli, J. Lightwave Technol. 20 (2002) 296.
[7] Q. Chen, Y.-D. Yang, Y.-Z. Huang, Opt. Lett. 32 (2007) 967.
[8] S. Xiao, M.H. Khan, H. Shen, M. Qi, Opt. Express 15 (2007) 14765.
[9] B.-S. Song, T. Asano, Y. Akahane, Y. Tanaka, S. Noda, J. Lightwave Technol. 23 (2005) 1449.
[10] A.S. Jugessur, P. Pottier, R.M. De La Rue, Opt. Express 12 (2004) 1304.
[11] Y. Akahane, T. Asano, H. Takano, B.-S. Song, Y. Takana, S. Noda, Opt. Express 13 (2005) 2512.
[12] B. Saadany, M. Malak, M. Kubota, F. Marty, Y. Mita, D. Khalil, T. Bourouina, IEEE J. Sel. Top. Quantum Electron. 12 (2006) 1480.
[13] A. Shinya, S. Mitsugi, E. Kuramochi, M. Notomi, Opt. Express 14 (2006) 12394.
[14] X. Shi, W. Ding, D.W.E. Allsopp, J. Lightwave Technol. 25 (2007) 2206.
[15] Y. Akahane, T. Asano, B. Song, S. Noda, Nature 425 (2003) 944.
[16] H.A. Haus, Y. Lai, J. Lightwave Technol. 10 (1992) 57.
[17] K.O. Hill, G. Meltz, J. Lightwave Technol. 15 (1997) 1263.
[18] Y. Yi, P. Bermel, K. Wada, X. Duan, J.D. Joannopoulos, L.C. Kimerling, Appl. Phys. Lett. 81 (2002) 4112.
[19] A. Lipson, Eric.M. Yeatman, Opt. Lett. 31 (2006) 395.
[20] P. Velha, J.C. Rodier, P. Lalanne, J.P. Hugonin, D. Peyrade, E. Picard, T. Charvolin, E. Hadji, New J. Phys. 8 (2006) 204.
[21] Q. Chen, M.D. Archbold, D.W.E. Allsopp, IEEE J. Quantum Electron., submitted for publication.
[22] R. Zengerle, O. Leminger, J. Lightwave Technol. 13 (1995) 2354.
[23] D.M. Beggs, M.A. Kaliteevski, S. Brand, R.A. Abram, J. Mod. Opt. 51 (2004) 437.
[24] A. Taflove, Advances in Computational Electrodynamics: The Finite-Difference Time-Domain Method, Artech House, Boston, MA, 1998.